Journal of Alloys and Compounds 726 (2017) 67–73

Contents lists available at ScienceDirect

Journal of Alloys and Compounds

journal homepage: http://www.elsevier.com/locate/jalcom

# Scintillation and TSL properties of $MgF_2$ transparent ceramics doped with $Eu^{2+}$ synthesized by spark plasma sintering

Fumiya Nakamura [a, *], Takumi Kato [a], Go Okada [a], Noriaki Kawaguchi [a], Kentaro Fukuda [b], Takayuki Yanagida [a]

[a] Nara Institute of Science and Technology (NAIST), 8916-5 Takayama-cho, Ikoma-shi, Nara, 630-0192, Japan
[b] Tokuyama Corporation, 1-1 Mikage-cho, Shunan-shi, Yamaguchi, 745-8648, Japan

ARTICLE INFO

*Article history:*
Received 28 April 2017
Received in revised form
4 July 2017
Accepted 29 July 2017
Available online 2 August 2017

*Keywords:*
Transparent ceramic
$MgF_2$
Scintillator
Dosimeter
Eu

ABSTRACT

We have developed $MgF_2$:Eu transparent ceramics using spark plasma sintering (SPS) and investigated the photoluminescence (PL), scintillation and dosimeter properties. Under X-ray irradiation, intense peaks appeared at 390 and 430 nm in all the samples. They were attributed to the 5d-4f transitions of $Eu^{2+}$ and some kinds of defect centers generated by doping with $Eu^{2+}$, respectively. The scintillation decay times of the emissions at 430 nm for the 0.01, 0.02, 0.05 and 0.1% Eu-doped samples were 21.1, 20.9, 18.6 and 23.4 ms, respectively. Furthermore, all the samples showed a thermally stimulated luminescence (TSL) over 120–250 °C. The TSL response was very sensitive to irradiation dose and showed a good linearity from 0.01 mGy to 100 mGy. The TSL emission measured at 170 °C was only by the luminescence band at 430 nm due to defect centers.



## 1. Introduction

Scintillators and dosimeters are used to measure ionizing radiations, and they have been put into use in various fields such as high energy physics [1], security [2], medicine [3] and protection dosimetry [4]. The scintillator converts incident radiation energy immediately into numerous low energy photons, and then they are further converted to electrical signal by a conventional photodetector. In contrast, a phosphor material used for dosimetry applications, or so-called dosimeter, stores radiation-generated electrons and holes at localized trapping centers. The trapped electrons and holes can be intentionally released out by an external stimulation of light or heat, and the charges eventually recombine to emit light. The resultant luminescence by light and heat stimulation is called optically stimulated luminescence (OSL) and thermally-stimulated luminescence (TSL), respectively. Dosimeters have been often used in personal dose monitoring applications, utilizing the storage luminescence signal as a probe of radiation dose accumulated over a period of time. Important characteristics of dosimeter material include low effective atomic number ($Z_{eff}$) which is close to that of soft tissue of human body ($Z_{eff}$ = 7.51) and linear response to the incident radiation dose. In practical applications, $Al_2O_3$ doped with C [5] and LiF doped with Ti, Mg [4] are used for OSL and TSL, respectively. It is required to study both scintillation and dosimeter properties in one material for better understanding of radiation-induced luminescence because we recently experimentally demonstrated that these properties are complementarily related [6,7].

Fluorides have attracted much attention as dosimeter materials [8–10]. Dosimeter properties of magnesium fluorides ($MgF_2$) doped with luminescent ions have been studied [11,12]. In addition, the effective atomic number of $MgF_2$ is very close to that of biological tissue. Therefore, the $MgF_2$ is a promising host for dosimeter materials. $MgF_2$ doped with $Eu^{2+}$ ($MgF_2$:Eu) has been studied as a phosphor material because it shows emission due to the 5d-4f transitions of $Eu^{2+}$ [13–15]. Despite the large number of research articles available on luminescence properties of $MgF_2$, most studies are on bulk single crystals and there are no reports on a transparent ceramic form and with Eu-doping. In our previous research, it has been shown that some luminescence properties induced by ionizing radiation were improved in a transparent ceramic form compared with those of single crystal [16,17]. Furthermore, transparent ceramics have some preferable properties over single

* Corresponding author.
*E-mail address:* nakamura.fumiya.nz9@ms.naist.jp (F. Nakamura).

http://dx.doi.org/10.1016/j.jallcom.2017.07.320
0925-8388/

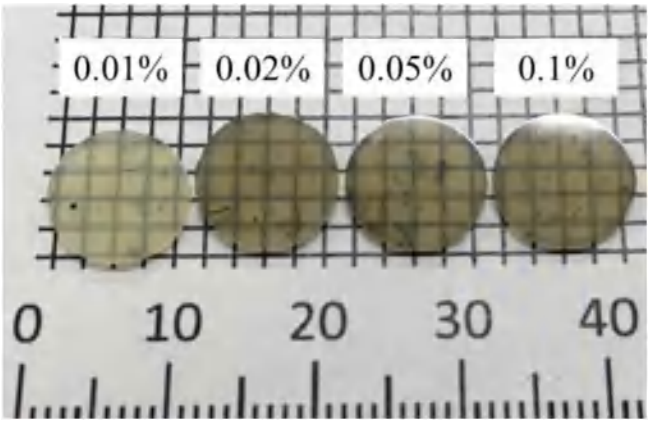


**Fig. 1.** Synthesized $MgF_2$ transparent ceramics doped with $Eu^{2+}$ (0.01, 0.02, 0.05 and 0.1%).

crystals for practical applications such as enhanced uniformity, high mechanical strength and low fabrication cost. For these reasons, we synthesized $MgF_2$:Eu transparent ceramics using spark plasma sintering (SPS) and evaluated the scintillation, photoluminescence (PL) and dosimeter properties. Applications of transparent ceramics are not limited to radiation detections but lasers [18–20], optics [21], persistent luminescence [22].

## 2. Experimental

A series of $MgF_2$:Eu transparent ceramic samples with different Eu concentrations (0.01, 0.02, 0.05 and 0.1 at.%) were synthesized by spark plasma sintering. A mortar and pestle was used to mix $MgF_2$ (4N) and $EuF_3$ (3N) raw powders. The mixture was loaded in a cylindrical graphite die with a hole with a diameter of 10.4 mm and held between two graphite punches inserted. Subsequently, the mixture was sintered by applying uniaxial pressure and supplying pulse current across the graphite assembly in an SPS furnace (LabX-100, Sinter Land). The temperature was elevated from the room temperature to 500 °C at a heating rate of 100 °C/min under 6 MPa pressure and then kept for 10 min. Next, the temperature was further elevated to 650 °C at a heating rate of 10 °C/min under 70 MPa pressure and then kept for 15 min. During the synthesis, the sample temperature was monitored using a K-type thermocouple attached on the graphite die. These sintering sequences in fact followed after those we have derived earlier to obtain transparent ceramics of $CaF_2$ by the SPS method [23,24]. Wide surfaces of the obtained ceramic samples were polished using a polishing machine (MetaServ 250, BUEHLER), and they were characterized by the following procedures.

A scanning electron microscope (SEM; Hitachi TM6600) was used to observe backscattered electron images. Optical in-line transmittance was measured using a spectrometer (V670, JASCO) over a spectral range of 190–2700 nm with 1 nm interval. Quantaurus-QY (C11347, Hamamatsu Photonics) was used to evaluate photoluminescence (PL) emission and excitation spectra as well as quantum yields. Quantaurus-τ (C11367, Hamamatsu Photonics) was used to measure PL decay profiles monitoring at 390 nm during 365 nm excitation.

X-ray induced scintillation spectrum was measured using our original setup [17]. For the X-ray source, a conventional X-ray tube (XRB80P&N200X4550, Spellman) equipped with a tungsten anode target and beryllium window was used. The generator was operated with a tube voltage of 40 kV and current of 5.2 mA. A 2.0 m optical fiber was used to guide the scintillation photons from the sample to a spectrometer (Andor DU-420-BU2 CCD and Shamrock 163 monochromator). Here, in order to avoid X-rays directly striking onto the CCD, the spectrometer was placed off the irradiation geometry axis. The spectrometer was cooled down to 193 K by a Peltier module to reduce the thermal noise. Furthermore, X-ray induced scintillation decay time and afterglow profiles were measured using a pulse X-ray source equipped afterglow characterization system [25]. The supplied X-ray tube voltage was 30 kV.

TSL glow curve was measured by a TSL reader (TL-2000,

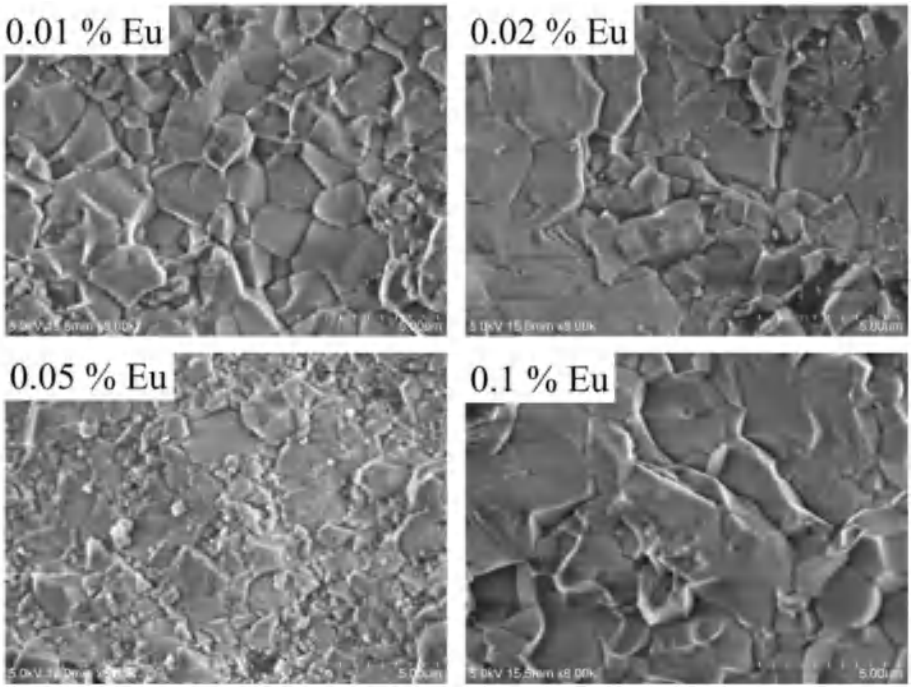


**Fig. 2.** SEM images of $MgF_2$ transparent ceramic samples doped with 0.01, 0.02, 0.05 and 0.1% $Eu^{2+}$.

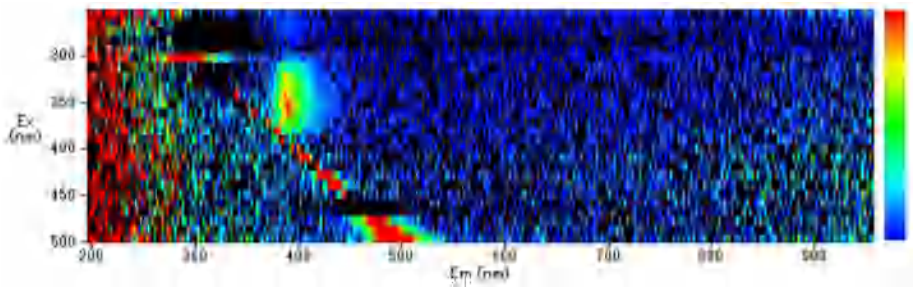

**Fig. 3.** PL emission and excitation map of 0.1% Eu-doped $MgF_2$ transparent ceramic sample.

Nanogray Inc.) over a temperature range of 50–490 °C with a heating rate of 1 °C/s [26]. Prior to the measurement, the sample was irradiated with X-rays of varying doses from 0.01 mGy to 100 mGy. In order to measure a TSL spectrum, an irradiated sample was heated at a specific temperature on a ceramic heater system (SCR-SHQ-A, Sakaguchi) and the luminescence was measured by a spectrometer (QE Pro, Ocean Optics). For the latter measurement, irradiation was performed with a conventional X-ray tube (XRB80P&N200X4550, Spellman) with a tube voltage of 80 kV and current of 2.5 mA for 10 min (which yield approximately 20 Gy).

## 3. Results and discussion

### 3.1. Sample

Fig. 1 shows a photograph of the $MgF_2$:Eu transparent ceramic samples made in this research. The samples are optically transparent enough that the black lines on the back of the samples were seen. The thickness of the 0.01, 0.02, 0.05 and 0.1% Eu-doped samples were 0.99, 1.15, 1.03 and 0.93, respectively. The varying thicknesses arose from the fact that the polishing was done individually for each sample by hand. Fig. 2 shows the SEM image of fractured surfaces of the samples. The average grain size of the 0.01, 0.02, 0.05 and 0.1% Eu-doped samples were about 1.77, 1.84, 1.82 and 2.03 μm. No significant difference of the grain sizes by doping concentration was seen in the SEM images.

### 3.2. Optical properties

PL excitation/emission contour graph of $MaF_2$:0.01% Eu transparent ceramic sample is shown in Fig. 3 as a representative. An intense broad emission band around 390 nm appeared under excitation around 350 nm. The origin of this emission would be ascribed to the 5d-4f transitions of $Eu^{2+}$, but the peak position of this emission was 50 nm shorter than that of earlier study of $MgF_2$:Eu single crystal [13]. However, the PL decay time of this emission was the typical value of the 5d-4f transitions $Eu^{2+}$ as described later, so this emission peak should be attributed to the 5d-4f transitions of $Eu^{2+}$. There was no large influence on the excitation and emission spectra affected by the Eu concentrations. The quantum yields of the 0.01, 0.02, 0.05 and 0.1% Eu-doped samples were 4.3, 0.7, 0.5 and 0.5%, respectively, and the sample with the lowest concentration of Eu (0.01%) showed the highest PL quantum yield.

Fig. 4 shows PL decay profiles of the $MgF_2$:Eu transparent

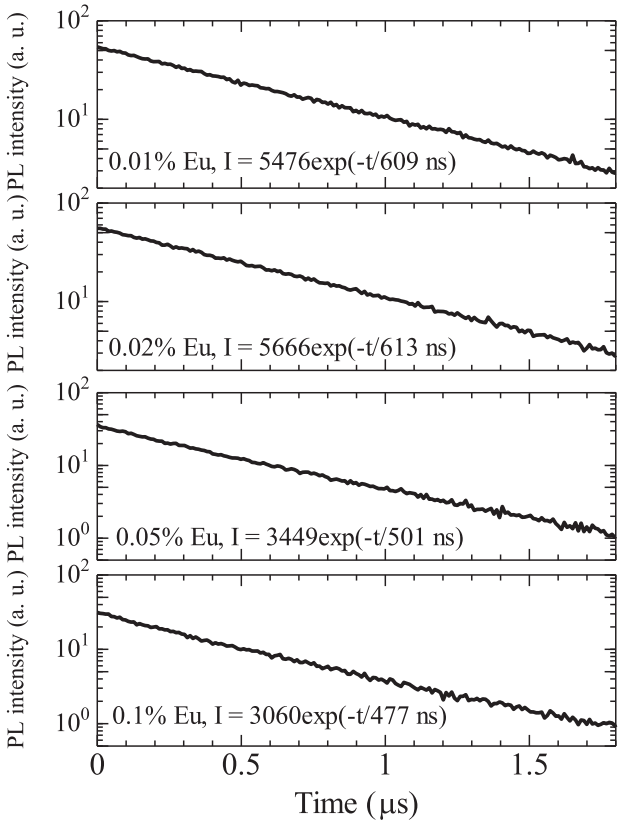


**Fig. 4.** PL decay profiles of $MgF_2$ transparent ceramics doped with different concentrations of $Eu^{2+}$. The monitoring wavelength was 400 nm while the excitation wavelength was 365 nm.

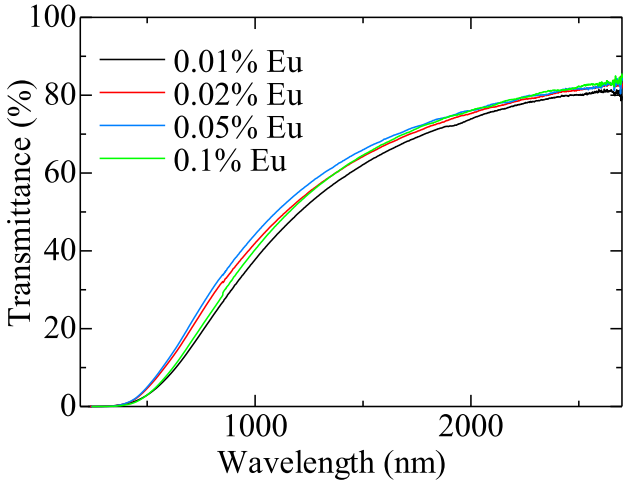


**Fig. 5.** Transmittance spectra of $MgF_2$ transparent ceramics doped with different concentrations of $Eu^{2+}$.

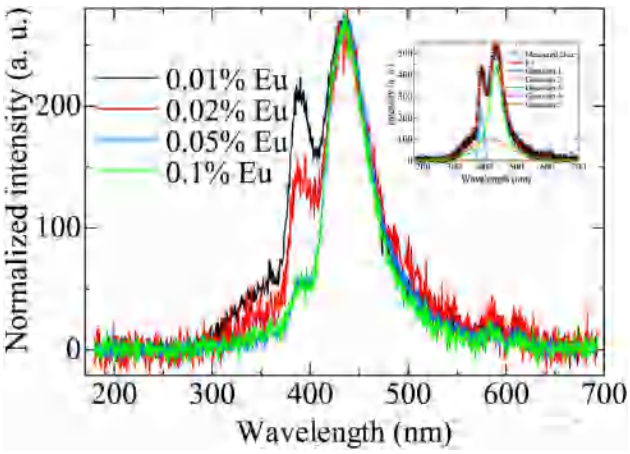


**Fig. 6.** X-ray induced scintillation spectra of $MgF_2$ transparent ceramics doped with different concentrations of $Eu^{2+}$. The inset shows the spectrum of the 0.01% Eu-doped sample superposed with Gaussian functions.

ceramic samples. The excitation wavelength was 365 nm while the emission at 390 nm was monitored during the measurement. These decay curves were well-approximated by single exponential decay function. The obtained decay time constants of the 0.01, 0.02, 0.05 and 0.1% Eu-doped samples were approximately 609, 613, 501 and 477 ns, respectively. These values were typical for the 5d-4f transitions of $Eu^{2+}$ [27].

In-line transmittance spectra of the $MgF_2$:Eu transparent ceramic samples are shown in Fig. 5. No clear correlation between the transmittance and Eu concentration was observed. This is consist with observations in the SEM images since a volume fraction of scattering centers such as grain boundaries and voids strongly affects the in-line transmittance. The strong absorption in the ultraviolet and visible ranges should be attributed to Mie scatterings due to grain boundaries, the 4f-5d transitions $Eu^{2+}$ and some kinds of defects.

### 3.3. Scintillation properties

X-ray induced scintillation spectra of $MgF_2$:Eu transparent ceramic samples are shown in Fig. 6. The inset shows the spectrum of the 0.01% Eu-doped sample which is fitted by Gaussian functions. Intense emission peaks appeared at 390 and 430 nm in all the samples in addition to a broad peak over 300–600 nm. The emission peak at 390 nm was attributed to the 5d-4f transitions of $Eu^{2+}$ as for the PL. In our previous study, the same broad emission over 300–600 nm was also observed in a non-doped $MgF_2$ transparent ceramic, and the origin should be some kinds of defect centers [28]. The intense peak at 430 nm was not seen in the non-doped $MgF_2$ transparent ceramic, and the emission peak due to $Eu^{2+}$ appeared near 430 nm in the earlier study of $MgF_2$:Eu single crystal [13]. However, this emission should not be due to $Eu^{2+}$ in these samples because if it were due to $Eu^{2+}$, it would be observed in the PL emission spectra. In these samples, the emission peak due to $Eu^{2+}$ was observed at 390 nm. Therefore, the origin of this peak should be due to some kinds of defect center generated by doping with $Eu^{2+}$. In addition, all the samples showed some weak peaks around 600 nm. The possible origins are the 4f-4f transitions of $Eu^{3+}$ or M ($C_1$) center [29,30]. The intensity ratio of the peak at 390 nm to the one at 430 nm decreased with an increase in the concentration of Eu. This behavior can be explained by concentration quenching of $Eu^{2+}$ ion, which was also observed as a decrease in the PLQY with increasing the concentration of $Eu^{2+}$.

X-ray induced scintillation decay time profiles of the $MgF_2$:Eu transparent ceramic samples are represented in Fig. 7. The top and bottom figures show the profiles measured over the ranges of 0–10 μs and 0–50 ms, respectively. In the shorter time range, all the

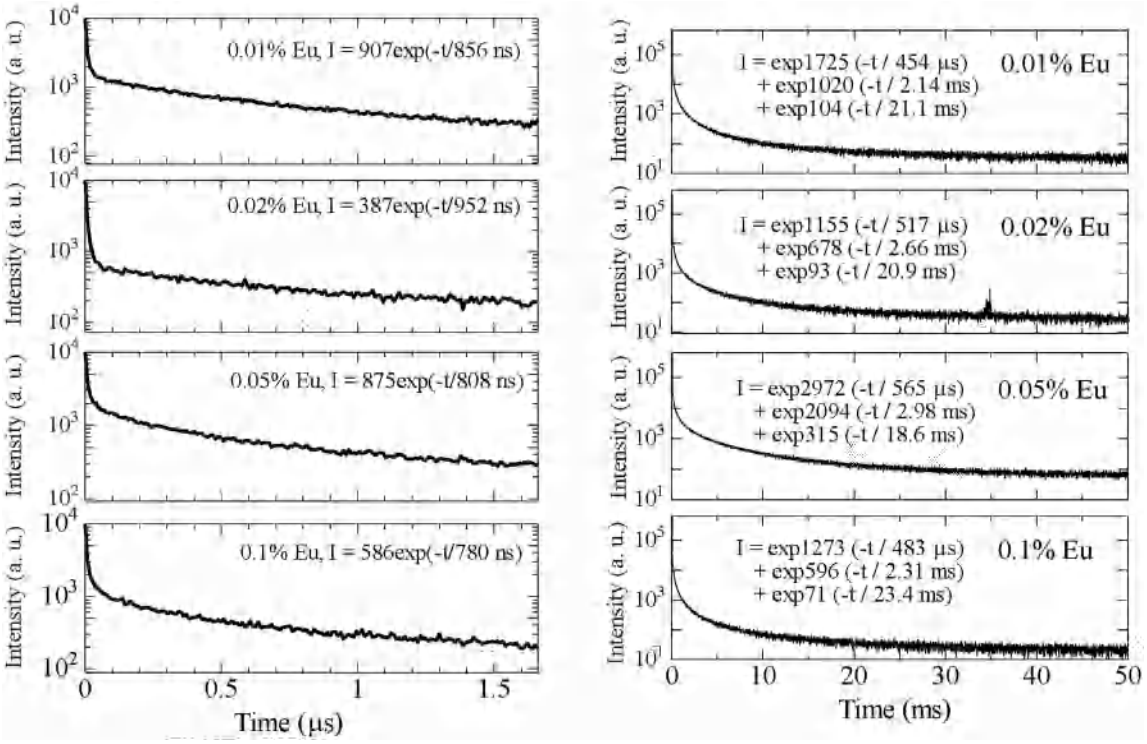


**Fig. 7.** Scintillation decay time profiles of $MgF_2$ transparent ceramics doped with different concentrations of $Eu^{2+}$. The top and bottom sets of figures show the profiles over the time ranges of 0–10 μs and 0–50 ms, respectively.

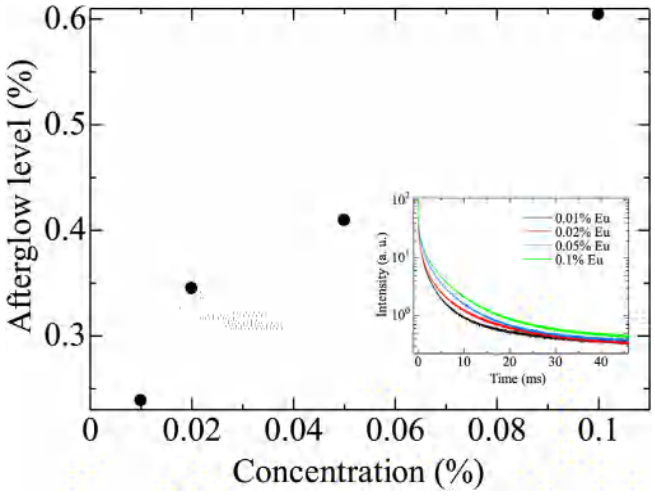


**Fig. 8.** Afterglow levels of $MgF_2$ transparent ceramics as a function of $Eu^{2+}$ concentration. The inset shows the afterglow profiles of all the samples.

decay curves were approximated by single exponential decay function. The faster decay constants of the 0.01, 0.02, 0.05 and 0.1% Eu-doped samples were 856, 952, 808 and 780 ns, and they were typical value of the 5d-4f transitions of $Eu^{2+}$. These decay times were slower than those of PL because scintillation mechanism involves energy transfer processes in addition to luminescence (excitation and emission as in PL) processes. All the decay curves measured in the longer time range were approximated by triple exponential decay function. The fastest decay time constants of the 0.01, 0.02, 0.05 and 0.1% Eu-doped samples were 454, 517, 565 and 483 μs, respectively. The second fastest decay times were 2.14, 2.66, 2.98 and 2.31 ms, respectively. The decay times of the fastest and second fastest components were also observed in non-doped $MgF_2$ transparent ceramic, so the origins were ascribed to the broad peak over 300–600 nm [28]. The slowest decay times of the 0.01, 0.02, 0.05 and 0.1% Eu-doped samples were 21.1, 20.9, 18.6 and 23.4 ms, respectively; and such slow signals were not observed in the non-doped $MgF_2$ transparent ceramic. From these results, it was suggested that the slowest component could be due to the emission at 430 nm. Although the 4f-4f transitions of $Eu^{3+}$ or M ($C_1$) center appeared in the scintillation spectra, this decay time was not detected as its intensity was too low. The slowest decay time was not observed in the PL although we tried to observe with several conditions. This may be because the excitation wavelength was shorter than the shortest wavelength available on the instrument, or the intensity was too low to be measured in our PL instruments.

Afterglow levels of the $MgF_2$:Eu transparent ceramic samples are represented in Fig. 8. The inset represents the afterglow profiles. Here, the afterglow level ($I_{AG}$) was defined as $I_{AG}(\%) = 100 \times (I_2 - I_{BG})/(I_1 - I_{BG})$ where $I_{BG}$ is the background signal intensity, $I_1$ is the averaged signal intensity during X-ray irradiation, and $I_2$ is the signal intensity at 20 ms after the irradiation was cut off [31]. The afterglow levels of the 0.01, 0.02, 0.05 and 0.1% Eu-doped samples at 20 ms showed 0.24, 0.34, 0.41 and 0.61%, respectively. The afterglow levels increased as the concentration of Eu increased.

### 3.4. Dosimeter properties

TSL glow curves of $MgF_2$:Eu transparent ceramic samples measured after X-ray irradiation are shown in Fig. 9. Here, the irradiation dose was fixed to 100 mGy for all the measurements. All the samples showed a major glow peak over 120–250 °C, and it was consistent with an earlier work with nanocrystalline $MgF_2$ [15]. The TSL intensity increased as the concentration of Eu increased. Fig. 10 represents TSL emission spectra measured at 170 °C. An intense emission peak was observed at 430 nm in all the samples. The same spectral features were seen in the scintillation spectra due to some kinds of defects, and we expect the same origin for the emission in TSL. Interestingly, the emission by $Eu^{2+}$ was not observed in TSL.

Fig. 11 shows TSL dose response curves of the $MgF_2$:Eu transparent ceramic samples as a dosimeter property. Here, the integrated TSL signal only for the peak at 170 °C was dealt for the TSL response. All the samples were sensitive to irradiation dose, and they showed a good linearity from 0.01 mGy to 100 mGy. This is an equivalent sensitivity with commercial personal dosimeters since the detection limit of typical commercial dosimeters for personnel dose monitoring applications is 0.1 mGy [32].

## 4. Conclusions

We have synthesized $MgF_2$:Eu transparent ceramics by SPS and investigated the PL, scintillation and dosimeter properties. Under X-ray irradiation, intense emission peaks appeared at 390 and

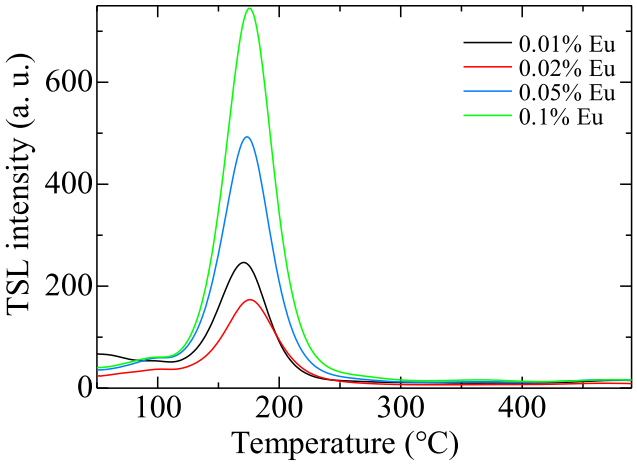


**Fig. 9.** TSL glow curves of $MgF_2$ transparent ceramic doped with $Eu^{2+}$ after 100 mGy X-ray irradiation.

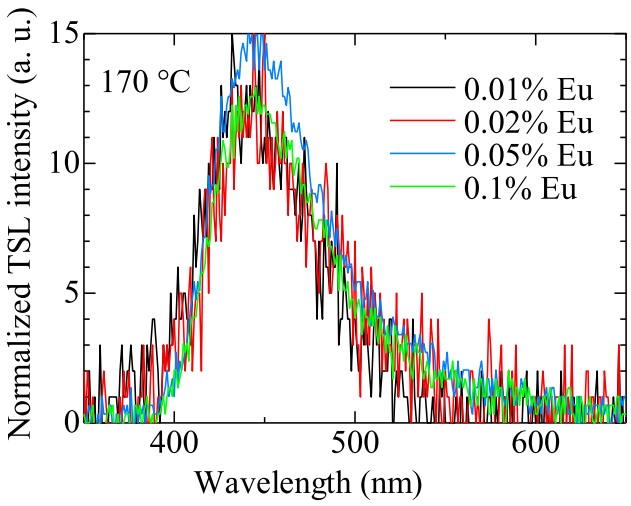


**Fig. 10.** TSL emission spectra of $MgF_2$ transparent ceramics doped with different concentrations of $Eu^{2+}$ measured at 170 °C. The samples were irradiated to approximately 20 Gy prior to the measurement.

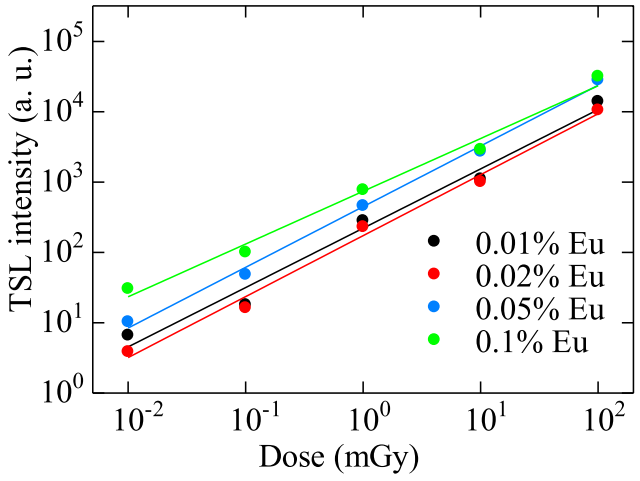


**Fig. 11.** TSL dose response curves of $MgF_2$ transparent ceramics doped with different concentrations of $Eu^{2+}$.

430 nm regardless the concentration of Eu. These emission origins were attributed to the 5d-4f transitions of $Eu^{2+}$ and some kinds of defect centers generated by doping with $Eu^{2+}$, respectively. The scintillation decay times of the emission at 430 nm of the 0.01, 0.02, 0.05 and 0.1% Eu-doped samples are 21.1, 20.9, 18.6 and 23.4 ms, respectively. In dosimeter properties, all the samples showed TSL glow peaks over 120–250 °C. They were very sensitive to irradiation dose and showed a good linearity from 0.01 mGy to 100 mGy. The TSL spectra measured at 170 °C indicated that the TSL active emission center was mainly defects, and no emission from $Eu^{2+}$ was observed.

## Acknowledgements

This work was supported by a Grant in Aid for Scientific Research (A)-26249147 and a Grant-in-Aid for Research Activity Start-up (15H06409) from the Ministry of Education, Culture, Sports, Science and Technology of the Japanese government (MEXT) as well as A-STEP and Matching Planner Program from Japan Science and Technology Agency (JST). The Cooperative Research Project of Research Institute of Electronics, Shizuoka University, KRF foundation, Murata Science Foundation, Hitachi Metals Materials Science foundation and Inamori foundation are also acknowledged.

## References

[1] T. Takahashi, K. Abe, M. Endo, Y. Endo, Y. Ezoe, Y. Fukazawa, M. Hamaya, S. Hirakuri, S. Hong, M. Horii, H. Inoue, N. Isobe, T. Itoh, N. Iyomoto, T. Kamae, D. Kasama, J. Kataoka, H. Kato, M. Kawaharada, N. Kawano, K. Kawashima, S. Kawasoe, T. Kishishita, T. Kitaguchi, Y. Kobayashi, M. Kokubun, J. Kotoku, M. Kouda, A. Kubota, Y. Kuroda, G. Madejski, K. Makishima, K. Masukawa, Y. Matsumoto, T. Mitani, R. Miyawaki, T. Mizuno, K. Mori, M. Mori, M. Murashima, T. Murakami, K. Nakazawa, H. Niko, M. Nomachi, Y. Okada, M. Ohno, K. Oonuki, N. Ota, H. Ozawa, G. Sato, S. Shinoda, M. Sugiho, M. Suzuki, K. Taguchi, H. Takahashi, I. Takahashi, S. Takeda, K.-I. Tamura, T. Tamura, T. Tanaka, C. Tanihata, M. Tashiro, Y. Terada, S. Tominaga, Y. Uchiyama, S. Watanabe, K. Yamaoka, T. Yanagida, D. Yonetoku, Hard X-ray detector (HXD) on board Suzaku, Publ. Astron. Soc. Jpn. 59 (2007) S35–S51, http://dx.doi.org/10.1093/pasj/59.sp1.S35.

[2] D. Totsuka, T. Yanagida, K. Fukuda, N. Kawaguchi, Y. Fujimoto, J. Pejchal, Y. Yokota, A. Yoshikawa, Performance test of Si PIN photodiode line scanner for thermal neutron detection, Nucl. Instrum. Methods Phys. Res. Sect. A Accel. Spectrom. Detect. Assoc. Equip. 659 (2011) 399–402, http://dx.doi.org/10.1016/j.nima.2011.08.014.

[3] T. Yanagida, A. Yoshikawa, Y. Yokota, K. Kamada, Y. Usuki, S. Yamamoto, M. Miyake, M. Baba, K. Kumagai, K. Sasaki, M. Ito, N. Abe, Y. Fujimoto, S. Maeo, Y. Furuya, H. Tanaka, A. Fukabori, T.R. Dos Santos, M. Takeda, N. Ohuchi, Development of Pr:LuAG scintillator array and assembly for positron emission mammography, IEEE Trans. Nucl. Sci. 57 (2010) 1492–1495, http://dx.doi.org/10.1109/TNS.2009.2032265.

[4] M.R. Mayhugh, R.W. Christy, N.M. Johnson, Thermoluminescence and color center correlations in dosimetry LiF, J. Appl. Phys. 41 (1970) 2968–2976, http://dx.doi.org/10.1063/1.1659346.

[5] S.W.S. McKeever, Optically stimulated luminescence: a brief overview, Radiat. Meas. 46 (2011) 1336–1341, http://dx.doi.org/10.1016/j.radmeas.2011.02.016.

[6] T. Yanagida, Ionizing radiation induced emission: scintillation and storage-type luminescence, J. Lumin 169 (2016) 544–548, http://dx.doi.org/10.1016/j.jlumin.2015.01.006.

[7] T. Yanagida, Y. Fujimoto, K. Watanabe, K. Fukuda, N. Kawaguchi, Y. Miyamoto, H. Nanto, Scintillation and optical stimulated luminescence of Ce-doped $CaF_2$, Radiat. Meas. 71 (2014) 162–165, http://dx.doi.org/10.1016/j.radmeas.2014.03.020.

[8] C. Sunta, A review of thermoluminescence of calcium fluoride, calcium sulphate and calcium carbonate, Radiat. Prot. Dosim. 8 (1984) 25–44. http://rpd.oxfordjournals.org/content/8/1-2/25.short.

[9] M.R. Mayhugh, Color centers and the thermoluminescence mechanism in LiF, J. Appl. Phys. 41 (1970) 4776, http://dx.doi.org/10.1063/1.1658540.

[10] W. Drozdowski, H.L. Oczkowski, Charge traps in Ce-doped $CaF_2$ and $BaF_2$, ACTA Phys. Pol. A 95 (1999). URI, http://repozytorium.umk.pl/handle/item/1916.

[11] M. Secu, C.E. Secu, S. Jipa, T. Zaharescu, M. Cutrubinis, High temperature thermoluminescence of $Mn^{2+}$-doped $MgF_2$ phosphor for personal dosimetry, Radiat. Meas. 43 (2008) 383–386.

[12] M. Secu, S. Jipa, C.E. Secu, T. Zaharescu, R. Georgescu, M. Cutrubinis, Processes involved in the high-temperature thermoluminescence of a $Mn^{2+}$-doped $MgF_2$ phosphor, Phys. Status Solidi Basic Res. 245 (2008) 159–162, http://dx.doi.org/10.1016/j.radmeas.2007.11.047.

[13] S. Lizzo, A.H. Velders, A. Meijerink, G.J. Dirksen, G. Blasse, The luminescence of $Eu^{2+}$ in magnesium fluoride crystals, J. Lumin. 65 (1995) 303–311, http://dx.doi.org/10.1016/0022-2313(95)00080-1.

[14] A.S. Ramírez-Duverger, R. Aceves, R. García-Llamas, J.A. Gaspar-Armenta, Europium luminescence enhancement induced by a resonant mode in a waveguide of planar metallic walls, J. Appl. Phys. 107 (2010) 053111, http://dx.doi.org/10.1063/1.3309839.

[15] L.G. Jacobsohn, A.L. Roy, C.L. McPherson, C.J. Kucera, L.C. Oliveira, E.G. Yukihara, J. Ballato, Rare earth-doped nanocrystalline $MgF_2$: synthesis, luminescence and thermoluminescence, Opt. Mater. 35 (2013) 2461–2464, http://dx.doi.org/10.1016/j.optmat.2013.06.045.

[16] T. Yanagida, K. Kamada, Y. Fujimoto, Y. Yokota, A. Yoshikawa, H. Yagi, T. Yanagitani, Scintillation properties of transparent ceramic and single crystalline Nd:YAG scintillators, Nucl. Instrum. Methods Phys. Res. Sect. A Accel. Spectrom. Detect. Assoc. Equip. 631 (2011) 54–57, http://dx.doi.org/10.1016/j.nima.2010.12.038.

[17] T. Yanagida, K. Kamada, Y. Fujimoto, H. Yagi, T. Yanagitani, Comparative study of ceramic and single crystal Ce:GAGG scintillator, Opt. Mater. 35 (2013) 2480–2485, http://dx.doi.org/10.1016/j.optmat.2013.07.002.

[18] E.H. Penilla, Y. Kodera, J.E. Garay, Simultaneous synthesis and densification of transparent, photoluminescent polycrystalline YAG by current activated pressure assisted densification (CAPAD), Mater. Sci. Eng. B Solid-State Mater. Adv. Technol. 177 (2012) 1178–1187, http://dx.doi.org/10.1016/j.mseb.2012.05.026.

[19] H. Yang, M. Omidalizarandi, X. Xu, I. Neumann, Terrestrial laser scanning technology for deformation monitoring and surface modeling of arch structures, Compos. Struct. 169 (2017) 173–179, http://dx.doi.org/10.1016/j.compstruct.2016.10.095.

[20] H. Yang, X. Wu, I. Neumann, Laser scanning-based updating of a finite-element model for structural health monitoring, IEEE. Sensors. J. 16 (2016) 2100–2104, http://dx.doi.org/10.1109/jsen.2015.25.08.965.

[21] U. Peuchert, Y. Okano, Y. Menke, S. Reichel, A. Ikesue, Transparent cubic-$ZrO_2$ ceramics for application as optical lenses 29 (2009) 283–291, http://dx.doi.org/10.1016/j.jeurceramsoc.2008.03.028.

[22] J. Xu, J. Ueda, K. Kuroishi, S. Tanabe, Fabrication of $Ce^{3+}$–$Cr^{3+}$ co-doped yttrium aluminium gallium garnet transparent ceramic phosphors with super long persistent luminescence, Scr. Mater. 102 (2015) 47–50, http://dx.doi.org/10.1016/j.scriptamat.2015.01.029.

[23] F. Nakamura, T. Kato, G. Okada, N. Kawaguchi, K. Fukuda, T. Yanagida, Scintillation and dosimeter properties of $CaF_2$ transparent ceramic doped with $Eu^{2+}$, Ceram. Int. 43 (2017) 604–609, http://dx.doi.org/10.1016/j.ceramint.2016.09.201.

[24] F. Nakamura, T. Kato, G. Okada, N. Kawaguchi, K. Fukuda, T. Yanagida, Scintillation and dosimeter properties of $CaF_2$ translucent ceramic produced by SPS, J. Eur. Ceram. Soc. 37 (2017) 1707–1711, http://dx.doi.org/10.1016/j.jeurceramsoc.2016.11.016.

[25] T. Yanagida, Y. Fujimoto, T. Ito, K. Uchiyama, K. Mori, Development of X-ray-induced afterglow characterization system, Appl. Phys. Express. 7 (2014) 8–11, http://dx.doi.org/10.7567/APEX.7.062401.

[26] T. Yanagida, Y. Fujimoto, N. Kawaguchi, S. Yanagida, Dosimeter properties of AlN, J. Ceram. Soc. Jpn. 121 (2013) 988–991, http://dx.doi.org/10.2109/jcersj2.121.988.

[27] C. Duan, A. Meijerink, R.J. Reeves, M.F. Reid, The unusual temperature dependence of the $Eu^{2+}$ fluorescence lifetime in $CaF_2$ crystals, J. Alloys Compd. 408–412 (2006) 784–787, http://dx.doi.org/10.1016/j.jallcom.2005.01.077.

[28] F. Nakamura, T. Kato, G. Okada, N. Kawaguchi, K. Fukuda, T. Yanagida,

Scintillation, TSL and RPL properties of $MgF_2$ transparent ceramic and single crystal, Ceram. Int. 43 (2017) 7211–7215, http://dx.doi.org/10.1016/j.ceramint.2017.03.009.
[29] P. Samuel, H. Ishizawa, Y. Ezura, K.I. Ueda, S. Moorthy Babu, Spectroscopic analysis of Eu doped transparent $CaF_2$ ceramics at different concentration, Opt. Mater. 33 (2011) 735–737, http://dx.doi.org/10.1016/j.optmat.2010.10.044.
[30] O.E. Facey, W.A. Sibley, Optical absorption and luminescence of irradiated $MgF_2$, Phys. Rev. 186 (1969) 926–932, http://dx.doi.org/10.1103/PhysRev.186.926.
[31] Nihon Kessyo Kogaku Co., Ltd. http://www.nk-k.co.jp/products/Detector.html, 2017 (accessed 17.03.28).
[32] From the homepage of Chiyoda Technol Corp. http://www.ctechnol.co.jp/radiation_monitoring/monitoring02, 2017 (accessed 17. 07. 04.) in Japanese.